

## Authors' response to Referee #1:

We would like to thank the referee for reviewing this manuscript, the valuable feedback and the very constructive comments. At this stage of the review process, we respond to the referee #1's comments and propose improvements for the final manuscript. The referee's original comments are printed in **bold** followed by the corresponding answers. Passages from the manuscript are printed in *italic writing*, in which proposed additions are indicated in blue and deleted parts in ~~red~~.

Thank you very much for your efforts,

Franz Mühle and Jan Bartl on behalf of all authors

---

### Specific comment (1)

With reference to the two bi-pole structures (contours of vertical wind speed behind the front rotor of test case 1, Fig. 8), it would be beneficial to add some discussion on the possible causes of these structures. The small-scale bi-pole structure seems to exist also behind the ForWIND turbine (test case 3, Fig. 15). It would be helpful to comment on whether such small-scale bi-pole only arises due to the wind tunnel environment, or whether, in certain conditions, it may also be observed in field operation.

Thank you for this very good comment. These bi-pole structures are indeed one of the most interesting features of these experiments and have recently been discussed in a number of publications by the authors (Bartl et al., 2018a; Schottler et al., 2018) and other research institutions (Howland et al., 2016; Vollmer et al., 2016; Bastankhah and Porte-Agel, 2016; Fleming et al., 2018; Berdowski et al., 2018). The discussion in the mentioned publications revealed that such structures are thought to establish for all scales, also for full-scale wind turbines in field operation.

The main purpose of the present paper is comparing the capability of different computational codes to simulate complex wake flows, without discussing the flow physics in detail. However, we suggest to add some more lines and references to the aforementioned sources in the text.

p.15, l.11 f:

*The wake contours as presented in Fig. 7b show a slightly curled wake shape, ~~which is generally well predicted by three of the simulations~~. The curled wake shape was shown to develop from a counter-rotating vortex pair, as discussed in detail by Schottler et al. (2018) and Bartl et al. (2018a) for the same experimental dataset. Similar flow physics behind a yawed turbine were observed in simulations by a full scale turbine by Howland et al. (2016) and Vollmer et al. (2016). The curled wake shape is generally well predicted by three of the simulations.*

### Specific comment (2)

With reference to the discussion on the wake characteristics of the downstream turbine (section 4.2.2.) it should be noted that the second turbine, impacted upon by the wake of the front turbine, will also generate 'its own wake', which in the absence of the oncoming wake of the upstream turbine, would not be deflected at all. Discussion and attempts to clarify the evolution of the resulting wake (strength, direction, etc.) behind the downstream rotor, in this reviewer's opinion, ought to acknowledge the existence of the aforementioned strongly nonlinear interaction, which is indeed very relevant to the application of these results to wind farm control by means of sacrificial turbines in the front row.

We appreciate this very good comment. We have specifically designed the second test case to be complex, i.e. the wake behind a non-yawed turbine exposed to the partial wake of a yawed upstream turbine. The results show a deflection of the wake behind the non-yawed downstream turbine as well, which is consistent with recent LES results presented by Fleming et al. (2018). The effects on power and yaw moments on the downstream turbine are presented in Bartl et al. (2018b).

Intentionally, we chose not to describe the complex flow physics of the test case in great detail. As mentioned above, our intention is to focus on comparing the capability of different computational codes to simulate complex wake flows. However, we agree with the reviewer, that a short discussion would add depth to this interesting flow phenomenon. We therefore suggest to add a couple of lines to the text:

p.18, l.9 f:

*T2 is located 3D behind the yawed upstream turbine, meaning that the wake flow of test case 1 represents the inflow for T2. Detailed results of power, thrust and yaw moments for the upstream and downstream turbine operated at different yaw angles, separation distances and inflow conditions are presented by Bartl et al. (2018b).*

p.20, l.13:

*This section discusses the wake characteristics 3D behind the two-turbine array. In this second test case the flow complexity is again increased, i.e. the wake behind a non-yawed turbine exposed to the partial wake of a yawed upstream turbine is investigated. The wake is clearly deflected in the negative z-direction. However, the deflection is not as big as 6D behind the single yawed turbine, but rather in the same range as 3D behind the single yawed turbine. This suggests that a further wake deflection is restricted by the non-yawed downstream turbine and maintained at approximately the same level, at which it hits the downstream turbine. These results compare well with a recent LES study by Fleming et al. (2018), who simulated a similar wake deflection behind a non-yawed downstream turbine exposed to a partial wake inflow.*

---

## Technical comment (1)

Readability could be improved by concluding Section Introduction with a clear overview of the article.

We agree that it would be beneficial to include an overview. Accordingly, short summary of the article's structure is suggested to be included at the end of the Introduction section:

p.3, l.4 f:

*By increasing the complexity with respect to previous Blind tests, the wake behind a yawed wind turbine is considered to be a challenging task for simulations. The work is organized as follows. Section 2 introduces the experimental setup including a presentation of the model wind turbines and the wind tunnel and inflow conditions as well as a description of the investigated test cases. Section 3 explains the methods used in the study, including descriptions of the measurement technique, the measurement uncertainty, the applied CFD codes and the methods used for comparison. In Section 4 the experimental results and the numerical predictions for power, thrust, yaw moments and wake characteristics are presented and compared. Section 5 discusses the findings of the study, before the conclusions are stated.*

## Technical comment (2)

At line 15 of section 2.1 it is stated that tip Reynolds number of the NTNU turbine is 110,000. It would appear that the reference velocity used for calculating this, is the absolute wind speed of 10 m/s (this is not stated in the paper and it probably should). At line 29 it is stated that S826 was designed for Reynolds about one order of magnitude higher. However, I think that the Reynolds of 1 million refers to relative wind speed whereas that at line 15 to absolute speed. The 2 differ by a factor of 6, implying that the operational Reynolds is much closer to the design one. Please comment/amend as appropriate.

Thank you for the comment, this might indeed be confusing and needs to be clarified. The Reynolds number of 110 000 for the NTNU turbine (line 15) and 64 000 for the ForWind turbine (line 26) were both calculated using the relative wind speed at the blade tip. The calculations are of the Reynolds numbers below.

The S826 airfoil was originally designed for higher Reynolds number of  $1.0 \times 10^6$  (as stated in line 29), but used at lower Reynolds numbers in the presented experiments. For clarification, we suggest to modify the corresponding lines in the text as follows:

p.3, l.29 f:

*It is designed for Reynolds numbers of  $Re=1.0 \times 10^6$ , which is around one order of magnitude higher as the Reynolds number at the rotor tip in the presented experiments. Nevertheless, experimental data sets for airfoil performance at the lower Reynolds range around  $Re=1.0 \times 10^5$  were measured ~~for lower Reynolds numbers~~ at Denmark's Technical University (DTU) ~~(Sarmast and Mikkelsen, 2012)~~ (Sarлак et al., 2018) and*

NTNU (Bartl et al., 2018c).

$$v_{\text{Re,NTNU}} = \sqrt{(10 \text{ m/s})^2 + (60 \text{ m/s})^2} = 60.83 \text{ m/s}$$

$$\text{Re}_{\text{NTNU}} = \frac{v_{\text{Re}} l_{\text{chord}}}{\nu} = \frac{60.83 \text{ m/s} * 0.026 \text{ m}}{1.46 * 10^{-5} \text{ m}^2/\text{s}} = 108\,327$$

$$v_{\text{Re,ForWind}} = \sqrt{(7.5 \text{ m/s})^2 + (45 \text{ m/s})^2} = 45.62 \text{ m/s}$$

$$\text{Re}_{\text{ForWind}} = \frac{v_{\text{Re}} l_{\text{chord}}}{\nu} = \frac{45.62 \text{ m/s} * 0.020 \text{ m}}{1.46 * 10^{-5} \text{ m}^2/\text{s}} = 62\,493$$

### Technical comment (3)

**Figure 3.** Since the oncoming flow is sheared, one should also indicate the orientation of the rotor angular speed because the turbine performance is in principle different depending on such sign. This information would be irrelevant only in the ideal case of zero wind shear. This information is only provided towards the end of the article, but it is suggested to add before the result section a clear schematic with the turbine, the three Cartesian axis and a graphical indication of the angular speed orientation.

Figure 3 is suggested to be complemented with the definition of the Cartesian axes and the rotational direction of the rotor. Furthermore, the rotational direction of the turbine is suggested to be added in the caption. See Figure 1 of this document.

### Technical comment (4)

**Caption of Fig. 4** starts with 'Inflow at different wind tunnel positions ...'. The word 'inflow', if I understand the figure correctly, may be misleading, because  $x/D > 0$  denotes positions downstream of the turbine, I assume? Please clarify/amend if required.

Thank you for pointing this out, this is indeed a misleading labeling. Actually, it is the flow measured in the empty wind tunnel. It is suggested to be changed in the caption to 'Vertical flow profiles in the empty wind tunnel at different positions, in which  $x/D = 0$  refers to the position, where the NTNU turbine is thereafter located'.

### Technical comment (5)

**Section 3.3.1, line 27:** please write time step as  $10^{-3}$  for clarity. It would also be useful to add comments on why this value was selected, and on

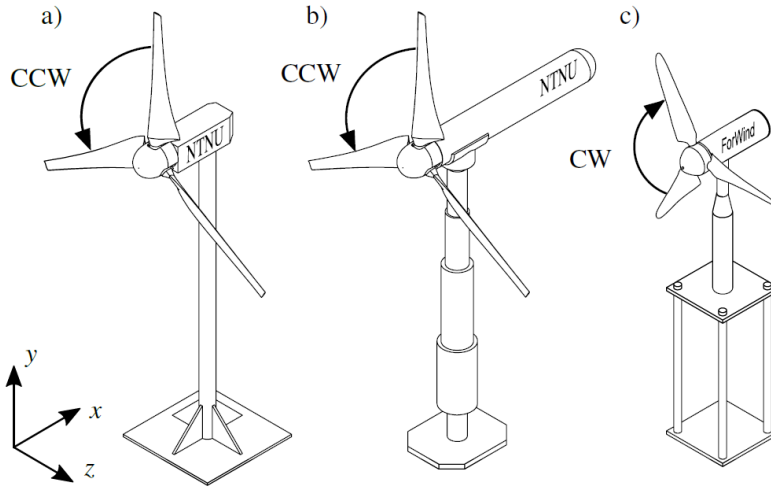


Figure 1: **Suggested version of Figure 3:** Sketches of the model wind turbines with reference coordinate system, (a) NTNU turbine LARS1 rotating in counterclockwise direction (CCW), (b) NTNU turbine T2 rotating in counterclockwise direction (CCW), (c) ForWind turbine rotating in clockwise direction (CW).

**mesh refinement analysis to ensure reasonable independence of the computed mean results on both the spatial and the temporal resolution. These comments should be added also for the other 3 CFD set-ups. It should also be indicated what percentage of the rotor period does this number correspond to. And also if the driving criterion for this choice was to allow the development of the upstream turbulence generated by the Synthetic eddy model.**

Thank you for this very constructive comment. These are indeed very important modeling parameters, that need to be included in the paper. In general, the modelers affirmed that their results are spatially and temporarily independent and have run corresponding sensitivity analyses.

The time step is changed to  $10^{-3}$  in section 3.3.1., line 27, as suggested. Also, the descriptions of all the CFD codes are suggested to be extended by explanations on the selection of the time step and the mesh refinement analysis. Table 2 is furthermore extended, now including the 'time step [s]' and 'recording interval [s]'.

p.8, l.12 ff:

*Siemens, who previously participated in Blind test experiments as CD-adapco, used the finite volume code STAR-CCM+ v12.04 to mesh and solve all three test cases. Each simulation resolved the rotor, nacelle and tower structure completely, and used the hybrid method Improved Delayed Detached Eddy Simulation (IDDES), which resolves the energy-carrying eddies in the free stream and solves the boundary layer flow with RANS. The Spalart-Allmaras model was used for closure of the turbulence equations, and the fluid was considered incompressible. Convective fluxes used a MUSCL 3<sup>rd</sup> order scheme, while time was discretized using a 2<sup>nd</sup> order implicit scheme. Each set of blades and hub was contained inside a cylindrical, rotating volume which was*

meshed with polyhedral cells, whereas the main domain used trimmed cells, resulting in a hexahedral dominant mesh in which a small proportion of cells was trimmed near the boundaries. Due to the rotation of the cylindrical volumes, the mesh was not conformal at the interface between the two regions, and flow quantities were interpolated from one volume to another. All wall surfaces, including the wind turbine bodies and the wind tunnel walls, were covered in several layers of prismatic cells to improve the resolution of boundary layers. The resulting  $y^+$  values were below 1 on the turbine bodies, and around 30 on the wind tunnel walls. The smallest cell size on the surface of the turbine bodies was 0.3 mm, typically found at the leading edge of the blades. The characteristic cell size in the rotating regions was 10 mm, which was also the cell size used in the wake of the rotors. The rest of the domain had a characteristic cell size of 20 mm. This resulted in meshes of  $29 \cdot 10^6$ ,  $35 \cdot 10^6$ , and  $17 \cdot 10^6$  cells for cases 1, 2, and 3 respectively. ~~All simulations were run with a time step of  $10^{-3}$  s. While a rigorous mesh dependency study was not performed, the mesh sizes were based on previous experience and expected to perform well with an affordable amount of cells. All simulations were run with a time step of  $1.0 \cdot 10^{-4}$  s, which was chosen to strike a balance between accuracy and computational cost. This value satisfies a number of criteria related to the rotation of the rotor regions. Namely, that the rotors turn by less than one degree per time step, and that the mesh is moved by only half the cell size at the interfaces between rotating regions and the rest of the domain. Furthermore, it was verified a posteriori that the convective Courant number virtually never exceeded 0.3 in the wake of the turbines. Admittedly, given the small cell size used to mesh the blades, the time step causes the blades to move by several cell sizes each time step, and the Courant number to well exceed 1, particularly so near the blade tips. While this limits the ability to resolve accurately the flow at the blades, it was deemed sufficient to produce accurate wake results. The computational domain matched exactly the test section as described in the invitation document, i.e. 11.15 m long and 2.71 m wide and the wind tunnel walls were included as no-slip wall boundaries. As inflow the given analytical mean velocity profile  $U_{inlet} = u_{ref} (y - y_{ref})^\alpha$  was used. Furthermore, the Synthetic Eddy Method was used to superpose time-dependent eddies with the characteristic length scale of 10 mm, and a turbulence intensity  $TI = 5\%$ . All cases were run for 1.6 s to establish the flow prior to sampling, and then mean values were sampled over a period of 2 to 3 s. An example using STAR-CCM+ can be found in Mendoca (2012).~~

p.9, l.2 ff:

*POLIMI submitted a LES that was computed using the ALEVM code. It is an aerodynamic turbine simulation tool written in C++ and based on pisoFoam, which is an incompressible transient solver included in the OpenFOAM framework. The standard PISO (Pressure-Implicit with Splitting of Operators) solver was modified to include the effect of the turbine blades that are represented using the lifting line approach. The blade lines are discretized in segments based on the intersections with the numerical mesh grid, in which an actuation point acts on each segment. Each point of the Actuator Line (ACL) acts as an isolated blade section. More information about the ACL method can be found in Sørensen and Shen (2002). The wind velocity is numerically sampled for every blade point and used to compute the relative wind speed and the angle of attack. Thereafter, the aerodynamic forces are obtained through a lookup table,*

in which the blades' geometrical and aerodynamic properties are listed. Dynamic stall effects are not considered. In ALEVM the wind velocity is not sampled on a single point but averaged over a line, which is placed upstream of the blade point position with a distance proportional to the mesh cell dimension. The wind velocity is estimated using the mean of the velocity probed across the line. The main purpose of the relative wind speed estimation is in the angle of attack calculation. The wind velocity direction is then corrected to account for the local up wash due to the lifting line force. Based on the lifting line approach, the ALEVM code includes the turbine blade effect as an external momentum source term in the Navier-Stokes equations solved by the PISO algorithm. ALEVM employs the well know solution of the Regularization kernel, smearing the line forces on the multiple cells following a Gaussian distribution and thus avoiding abrupt variation of the source term strength between adjacent cells. The turbulence in the wake region is modeled using a LES, adopting the Smagorinsky sub-grid scale model. For the time discretization scheme a first order implicit approximation is used, while the divergence discretization scheme and the gradient discretization scheme are approximated by second order. The simulation is run for a time interval of 20 s, while a time step of  $1.0 \cdot 10^{-3}$  s is used. This results in an angular rotation of about  $2.4^\circ$  per time step, which conversely means that 150 time steps make a full rotation. The resultant maximum Courant number of 0.21 is well below 1, indicating a sufficient temporal accuracy. The wind tunnel walls are included as no-slip-boundaries, while also the inlet turbulence grid is geometrically modeled. The total cell count for the simulations is approximately  $4.1 \cdot 10^6$ . Further details about the code can be found in Schito (2014).

p.10, l.2 ff:

UdelaR submitted another LES using their in-house developed *caffa3d* code. It is an open source, finite volume code, with second order accuracy in space and time, parallelized with a Message Passing Interface (MPI), in which the domain is divided in unstructured blocks of structured grids. Complex geometries are represented by a combination of body fitted grids and the immersed boundary method over both, Cartesian and body fitted grid blocks. The code is F90 and currently runs on CPU, while a CUDA GPU version is currently being developed. The properties of the geometry and the flow are expressed as primitive variables in a Cartesian coordinate system, using a collocated arrangement. An ACL approach is used to discretize the turbine blades in the simulations. The aerodynamic forces on the blade elements are computed using the provided XFOIL data, dynamic stall effects are not considered. The forces then are projected onto the computational domain. In order to compute the additional source term, a Gaussian smearing function is used, taking into account one smearing factor for each direction: normal, tangential and radial to the rotor plane. The domain, representing the wind tunnel ( $12.5D_{LARS1} \times 3D_{LARS1} \times 2D_{LARS1}$ ), is uniformly divided into  $192 \times 72 \times 48$  grid cells in the streamwise, spanwise and vertical directions, resulting in a total cell count of approximately  $0.7 \cdot 10^6$ . A zero velocity gradient is imposed at the outlet, while a logarithmic law is used to compute the stress at the bottom wall and the symmetry boundary condition is used at the lateral and top boundaries. ~~A~~ An implicit Crank-Nicolson time scheme is used with a time step of  $2.5 \cdot 10^{-3}$  s, that corresponds to 0.16 of the rotor period (similar temporal resolution where used before, see for instance Guggeri et al. (2017)). Both time step size and spatial resolution were defined based

on previous simulations performed by UdelaR, particularly of Blind Test 4. The scale dependent dynamic Smagorinsky model is used to compute the subgrid scale stress, using a local averaging scheme. The inflow condition is obtained from a precursor simulation with a similar numerical setup—, but without model wind turbines and using a periodic boundary condition at the West and East boundaries with a constant pressure gradient as forcing term. The upstream model wind turbine is placed  $2D_{LARS1}$  from the inlet boundary for test cases 1 and 2, while for test case 3 the model wind turbine is placed  $5D_{LARS1}$  from the inlet boundary. UdelaR results are obtained after averaging the simulated data over 52.5 s for test cases 1 and 2 and 67.5 s for test case 3. More information about the application of `caffa3d` for wind energy simulations can be found in Guggeri et al. (2017), Mendina et al. (2014) and Usera et al. (2008).

p.10, l.18 ff:

A third LES was submitted by KTH. The spectral element code `Nek5000` (Fischer et al., 2008), which was developed to solve the dimensionless, incompressible Navier–Stokes equations, was used. Each spectral element is discretized using Gauss–Lobatto–Legendre quadrature points on which the solution is expanded using Legendre polynomials. The LES applies a spatial filtering technique to the two highest modes to remove a part of the energy in the smallest scales and redistribute it to the lower modes thus stabilizing the numerical simulation. The domain is discretized using  $7.98 \cdot 10^4$  uniformly distributed spectral elements with ~~9<sup>th</sup>~~ 9<sup>th</sup> order polynomials in each element, resulting in a total cell count of approximately  $58 \cdot 10^6$ . The numerical domain size corresponds to the dimensions of the wind tunnel. In the case of the NTNU turbine this mesh size corresponds to 45 grid points along each blade, when the blades are aligned with the mesh. The distance between the inlet and the first turbine is 4 rotor radii and the total length of the domain corresponds to 25 rotor radii. The dimensionless time step used to advance the simulation is  $\delta_t = 1.5 \cdot 10^{-3}$  which corresponds to 0.1432% of a rotor revolution and is chosen to satisfy the Courant–Friedrichs–Lewy condition. The wind turbine blade geometry is represented by body forces according to the ACL method with the lift and drag forces being computed using tabulated airfoil data. For the NTNU turbines the experimental airfoil data set from DTU (Sarлак et al., 2018) is used. It provides lift and drag coefficients over a range of Reynolds numbers. The ForWind turbine lift and drag forcing was computed using airfoil polars generated by Xfoil that were provided in the invitation. Dynamic stall is not considered in the modeling approach. At the blade tips the Prandtl tip correction is applied. The forces computed at each actuator line are distributed using a three-dimensional Gaussian distribution. The Gaussian width is selected to be 2.5 times the average grid spacing. A mesh independency study of the unyawed NTNU wind turbine established that using the aforementioned domain resolution combined with this Gaussian width provided a converged averaged wake development. The tower is also modeled using a body force approach. Both an oscillating lift component and a constant and oscillating drag component are included. The lift and drag coefficients for the mean drag and root-mean-squared lift and drag of a cylinder are taken from Freso et al. (2011). The line forces are then distributed using the three-dimensional Gaussian approximately in the volume occupied by the tower. This setup has been previously validated against experimental data from the NTNU turbine (Kleusberg et al., 2017). In the case of the ForWind turbine only the actual tower of the support structure is included. The turbulence at the inlet is modeled using sinu-



Table 1: Overview of simulation methods and parameters. Abbreviations: Improved Delayed Detached Eddy Simulation (IDDES), Large Eddy Simulation (LES), Actuator Line (ACL), Fully Resolved (FR).

Participant	Simulation code	Flow solver type	Rotor model	Airfoil polars	Tower, nacelle	Mesh properties	Number of cells	Time step [s]	Recording interval [s]
Siemens	Star-CCM+	IDDES	FR	-	FR	Hexah./polyh.	$\approx 30.0 \cdot 10^6$	$1.0 \cdot 10^{-4}$	2 - 3
POLIMI	ALEVM	LES	ACL	X-Foil	No	Cartesian	$\approx 4.1 \cdot 10^6$	$1.0 \cdot 10^{-3}$	20
UdelaR	caffa3d	LES	ACL	X-Foil	Yes	Cartesian	$\approx 0.7 \cdot 10^6$	$2.5 \cdot 10^{-3}$	52.5 - 67.5
KTH	Nek5000	LES	ACL	Experiments	Yes	Uniform	$\approx 58.0 \cdot 10^6$	$1.5 \cdot 10^{-3}$	4 - 5.3

*soidal modes with random phase shifts and they are scaled with a von Kármán energy spectrum. It is superimposed to the desired uniform inflow condition. The turbulence is calibrated to give a turbulence intensity at hub height of approximately  $TI = 10.0\%$  at the upstream turbine LARS1 and  $TI = 4.8\%$  at the downstream turbine T2. At the outlet a zero-stress boundary condition is used while the symmetry boundary condition is imposed laterally to avoid resolving the wall boundary layer. More details about the the computational setup can be found in Kleusberg et al. (2017). The velocity and turbulent kinetic energy in the wake were temporally averaged over a dimensional time interval  $\Delta t = 4 - 5.3$  s, which corresponds to over three flow-throughs of the numerical domain in the NTNU cases.*

### Technical comment (6)

For clarity and to allow other research groups to use these results, it would be very useful to provide for each of the 4 sets of CFD simulations the distance of the inflow and outflow boundaries the distance from the first turbine along the direction of the wind stream.

Thank you for this comment. The distances are included in the updated descriptions of the CFD codes as presented above.

### Technical comment (7)

Section 3.3.5, line 12. I think it's 'moment', not 'moments'.

We think that the plural form moments is also correct here, as it refers to several values of the requested yaw moment for the different test cases . We referred to power coefficients, thrust coefficients and yaw moments.

### Technical comment (8)

First 2 lines of section 3.4.2 appear misplaced in that section.

We agree, the two lines confuse the reader and are not necessary. Therefore, we suggest to remove the first two lines of this section.

p.12, l.20 f:

~~The predictions of  $CP$ ,  $CT$  and  $My^*$  are directly compared to the experimental results. The deviations of the predictions from the measurements are presented as a percentage of the experimental reference value in supplementing tables.~~

### Technical comment (9)

Page 14, line 6: please provide clear definition of Angle of Attack in yawed wind or cite suitable reference.

This is a very good point. We used the same definition as in the non-yawed case, where the angle of attack is defined as the angle between the relative flow direction and the chord of the blade. However, the analysis of the angle of attack was not the main focus of this study. A deeper analysis of this is given by Morote (2016).

The goal of our 2-dimensional analysis is to show the angle of attack strongly varies in the course of one rotation, and to give estimates of which flow regime the airfoils might operated in. We agree, that we should mention this simplified approach in the text and therefore suggest the following additions:

p.14, l.6 ff:

*The calculations showed that the angle of attack for the yawed turbine is fluctuating about  $2.0^\circ$  during one rotation in the outer third of the blade, causing very high angles of attack ~~to occur on the blade~~. Note, that the definition of the angle of attack is herein based on a simplified two-dimensional analysis, which omits the lateral component in the relative velocity during yaw.*

### Technical comment (10)

Section 4.1.2. Please specify for both experimental data and numerical results whether the presented contours of streamwise velocity are averaged over a certain time interval or if they are instantaneous values. If they are averaged, please provide time interval.

All the data are time-averaged over a certain interval. For the experimental data, this is stated in section 3.3.6 and repeated in section 4.1.2. The time interval length is provided in chapter 3.1, indicating an average sampling time was approximately 25 - 33 s, depending on the non-constant data acquisition rate of the LDV system. The time interval used in the four numerical simulations is provided in the updated code descriptions (see further above in this document).

### Technical comment (11)

Figures 7a and 8a: are these lines at hub height? Or averages along vertical direction? Please specify.

Thank you for pointing this out. The wake profiles are measured at hub height. The

captions of Figures 7 – 16 are therefore completed by this information: ”Line plot at hub height...”.

### Technical comment (12)

Page 19, line 1: ’... and the TST ... 5 is computed using  $u_{ref} = 10m/s$ ’. This sentence is unclear.

Thank you for the comment. We think that it is important that we mention that the TSR of 5 for the downstream turbine was calculated using the reference velocity of 10 m/s and not the actual velocity in the wake. Nevertheless, we agree that the formulation of the sentence is unclear. Therefore, the sentence was divided into two sentences to make it clearer what we mean.

p.19, l.1 f:

*The downstream turbine T2 is operated at  $\gamma_{T2} = 0^\circ$  and  $\lambda_{T2} = 5.0$ . The tip speed ratio  $\lambda_{T2} = 5.0$  is computed using the far-upstream reference velocity  $u_{ref} = 10.0$  m/s.*

### Technical comment (13)

At page 26 (Discussion and conclusions) it is stated ‘The fourth simulation fully resolved the rotor geometry and directly calculated the forces on the rotor. The time-step in these simulations was chosen to be rather large in order to save computational time which might have negatively influenced the accuracy of the blade forces’. This statement presumably refers to the Siemens analyses, which used time step of 10-3 seconds. Why is this step considered small? With reference to what? Is it expected that the optimal time-step for a rotor resolved simulation should be smaller than for an ACL simulation? It would be very helpful to provide the value of the time-step for all 4 CFD simulation sets. As commented above, is the Siemens time-step too large for the synthetic eddy method although sufficient for resolving rotor unsteady aerodynamics ? Is this time-step deemed insufficient to resolve the wake turbulence? Comments on this would be very helpful to the wind farm CFD community.

Thank you for pointing this out. This is indeed an unclear and aslo incorrect description and needs revision. In Siemens’ simulations, not the time step is large, but the time interval is rather short (compared to the other simulations in this BT). This short time interval might not be sufficiently long to calculate the correct time-averaged blade forces. Nevertheless, the high computational cost for the fully-resolved Siemens setup allow only short simulations, which is considered to be a major drawback of this type of simulation. The values of the time step for all simulation are included in the individual code descriptions above and Table 2. The Conclusions are suggested to be modified as follows:

p.26, l.10 f:

*The experimental airfoil polars might be more realistic for such large angles of attack, which result in better performance predictions. The ~~fourth~~ IDDES simulation fully resolved the rotor geometry and directly calculated the forces on the rotor. The ~~time-step in these simulations~~ length of the simulation interval was chosen to be rather ~~large~~ short in order to save computational time ~~which might have negatively~~. This might have influenced the accuracy of the time-averaged blade forces. The parameters of the wake flow, however, were not ~~impaired by this large time-step~~ observed to be impaired by the short averaging interval.*

### Technical comment (14)

**The KTH simulation used measured lift and drag data. Was the maximum value of the angle of attack for which experimental data were available greater than the largest AoA expected in the 3D simulation? Or were empirical extrapolations used in the CFD look-up tables, similarly to what done in BEM analyses?**

According to the tables provided by Sarlak et al. (2018), angles of attack ranging from  $\alpha = -10^\circ$  to  $25^\circ$  were available from the experimental dataset. For actuator line codes, empirical extrapolations for higher (or lower) AoAs, similar to BEM codes, are used.

### Technical comment (15)

**The IDDES simulations used Synthetic Eddy Method to enforce turbulent inflow fluctuations. It should be specified, however, if the other three simulation sets did something similar or used instead steady inflow conditions.**

This is a very good comment, that mostly is answered in the updated descriptions of the simulation methods. Polimi actually fully resolved the turbulence and shear generating grid used in the experiment, while Udelar and KTH used a sinusoidal modes with random phase shifts scaled with a von Karman energy spectrum, and run a precursor simulation to match the experimentally measured inflow conditions.

## References

- [1] Bartl, J., Mühle, F., Schottler, J., Sætran, L., Peinke, J., Adaramola, M., and Hölling, M.: Wind tunnel experiments on wind turbine wakes in yaw: Effects of turbulence and shear, Wind Energy Sci., 3, 329-343, doi: 10.5194/wes-3-329-2018, 2018.

- [2] Schottler, J., Bartl, J., Mühle, F., Sætran, L., Peinke, J., and Hölling, M.: Wind tunnel experiments on wind turbine wakes in yaw: Redefining the wake width, *Wind Energy Sci.*, 3, 257-273, doi: 10.5194/wes-3-257-2018, 2018.
- [3] Howland, M., Bossuyt, J. Martinez-Tossas, L. Meyers, J. and Meneveau, C.: Wake structure in actuator disk models of wind turbines in yaw under uniform inflow conditions, *J. Renewable Sustainable Energy* 8, 043301, doi: 10.1063/1.4955091, 2016.
- [4] Vollmer, L., Steinfeld, G., Heinemann, D., and Kühn, M.: Estimating the wake deflection downstream of a wind turbine in different atmospheric stabilities: an LES study, *Wind Energy Science*, 1, 129–141, doi: 10.5194/wes-1-129-2016, 2016.
- [5] Bastankhah, M. and Porté-Agel, F.: Experimental and theoretical study of wind turbine wakes in yawed conditions, *Journal of Fluid Mechanics*, 806, 506–541, doi: 10.1017/jfm.2016.595, 2016.
- [6] Fleming, P., Annoni, J., Churchfield, M., Martinez, L., Gruchalla, K., Lawson, M., and Moriarty, P.: A simulation study demonstrating the importance of large-scale trailing vortices in wake steering, *Wind Energ. Sci.*, 3, 243-255, doi: 10.5194/wes-3-243-2018, 2018.
- [7] Berdowski, T., Ferreira, C. van Zuijlen, A. and van Bussel, G.: Three-Dimensional Free-Wake Vortex Simulations of an Actuator Disc in Yaw, *AIAA SciTech Forum, Wind Energy Symposium 2018*, doi: 10.2514/6.2018-0513, 2018.
- [8] Herges, T., Maniaci, D., Naughton, B., Mikkelsen, T., and Sjöholm, M.: High resolution wind turbine wake measurements with a scanning lidar, *Journal of Physics: Conf. Series* 854, 012021, doi: 10.1088/1742-6596/854/1/012021, 2017.
- [9] Bartl, J., Mühle, F., and Sætran, L.: Wind tunnel study on power output and yaw moments for two yaw-controlled model wind turbines, *Wind Energy Sci.*, 3, 489-502, doi: 10.5194/wes-3-489-2018, 2018.
- [10] Sarlak, H., Frere, A., Mikkelsen, R., and Sørensen, J.N.: Experimental Investigation of Static Stall Hysteresis and 3-Dimensional Flow Structures for an NREL S826 Wing Section of Finite Span, *Energies*, 11, 1418; doi:10.3390/en11061418, 2018.
- [11] Bartl, J., Sagmo, K., Bracchi, T. and Sætran, L.: Performance of the NREL S826 airfoil at low to moderate Reynolds numbers - A reference experiment for CFD models, *European Journal of Mechanics-B/Fluids*, in review, 2018.
- [12] Morote, J.: Angle of attack distribution on wind turbines in yawed flow, *Wind Energy*, 19 (4), 681–702, doi: 10.1002/we.1859, 2016.